NTATION PAGE

Form Approved
OBM No. 0704-0188

ate.	3. Report Type and Dates Covered.
March 20, 1993	Final - Contractor Report - April 1, 1989 - March 31, 1992

4. Title and Subtitle.
Profiling ALACE Instruments

5. Funding Numbers.
Contract N00014-89-C-6014
Program Element No. 0602435N
Project No. 03587
Task No. MOG
Accession No. DN259140
Work Unit No. 13210X

6. Author(s).
Jeff Sherman*

7. Performing Organization Name(s) and Address(es).
*Scripps Institution of Oceanography (PI - Russ E. Davis)
La Jolla, CA 92093-0230

8. Performing Organization Report Number.
N00014-89-C-6014

9. Sponsoring/Monitoring Agency Name(s) and Address(es).
Naval Research Laboratory
Ocean Sciences Branch
Stennis Space Center, MS 39529-5004

10. Sponsoring/Monitoring Agency Report Number.
NRL/CR/7330--93-0001

11. Supplementary Notes.
Not published, written only for final report.

12a. Distribution/Availability Statement.
Approved for public release; distribution is unlimited.

13. Abstract *(Maximum 200 words).*

The Autonomous Lagrangian Circulation Explorer (ALACE) is a free drifting oceanographic float which drifts at a level of neutral buoyancy and periodically rises to the surface where it transmits data to System Argos satellites and is located by them. The basic float was intended to observe ocean currents but recent developments, described in this report, have led to three new versions with expanded capabilities. One model reports temperature profiles from each ascent cycle. A second reports profiles of both temperature and conductivity from which sound speed profiles can be calculated. A third instrument observes microtemperature profiles on repeated vertical profiles and records them internally. At the end of its mission this float must be located from its Argos signals and recovered. All three floats have been field tested and their performances are discussed. The sound speed profiles obtained from the first conductivity and temperature until are accurate to 0.25 m/s after correcting for instrument drift using relatively stable climatological temperature vs salinity relations at depth. Subsequent sensor improvements are believed to have reduced drift.

14. Subject Terms.
Autonomous ocean measurement system, satellite data links, ocean profilers

15. Number of Pages.
27

16. Price Code.

17. Security Classification of Report.	18. Security Classification of This Page.	19. Security Classification of Abstract.	20. Limitation of Abstract.
Unclassified	Unclassified	Unclassified	SAR

NSN 7540-01-280-5500

Standard Form 298 (Rev. 2-89)
Prescribed by ANSI Std. Z39-18
298-102

Profiling ALACE Instruments

Jeff Sherman
Instrument Development Group
Scripps Institution of Oceanography
La Jolla, California

Three remote-profiling instruments have been developed, based on the Autonomous LAgrangian Circulation Explorer (ALACE), a neutrally-buoyant float used to track sub-surface currents. Profilers include two versions which measure temperature alone, or temperature and conductivity, on instrument's ascent. The data is transmitted through the Argos satellite system before ALACE descends again to its neutral depth. A third version measures temperature microstructure from two probes while descending, storing data to a 200 Mb hard disk. The instrument must be retrieved at the end of its deployment to recover the data. All three types have been deployed, and their performances are discussed.

1. Introduction

A neutrally-buoyant float has been recently developed to track sub-surface currents over a multi-year time span. The instrument, ALACE (Autonomous LAgrangian Circulation Explorer), is described by Davis et al.(1992). Tracking of the instrument's location is performed by it periodically rising to the surface, where position is located via the Argos satellite system. This vertical cycling allows additional information to be collected on ascent/descent, resulting in data-profiling ALACEs. This paper describes three such profilers that have been developed to date.

The profiling-temperature ALACE (PT-ALACE) records and averages temperature on ascent, and then transmits the data through Argos (section 2). The CTD-ALACE has in addition a conductivity sensor (section 3). The LAMP (Long-term ALACE Micro-temperature Profiler) is outfitted with two micro-temperature probes and a 200 mb hard disk. Unlike normal ALACEs, LAMP performs all of its cycles, and then, only at the end of its mission, transmits to Argos. LAMP is then retrieved and the data recovered (section 4).

The ALACE instrument is described by Davis et al.(1992). A quick overview is given here. ALACE is an autonomous float, ballasted to be neutrally-buoyant at a desired depth. The instrument is programmed to cycle on a set time basis. The cycle consists of the following steps (starting with ALACE already at its neutral depth): Oil is pumped into an external bladder, with the added buoyancy resulting in ALACE rising to the surface. ALACE transmits to Argos, which provides a fix on its position. After typically 24 hours on the surface, ALACE evacuates the bladder, descending to its original depth. The instrument remains at this depth until it is time to perform the next ascent (usually 10-25 days). This cycling continues until the batteries fail (on order 50 profiles). Differences in surface positions between cycles are used to estimate ocean currents at ALACE's neutral depth. The instrument consists of a .16 m diameter aluminum pressure case .94 m in length, with a .6 m long antenna attached to the semi-hemispherical top end cap. The bottom end cap contains an external bladder capable of holding 800 cc of oil.

2. PT-ALACE

The profiling temperature ALACE (PT-ALACE) represents the simplest extension of the basic ALACE design, with a temperature probe added to the top end cap. Existing analog and digital electronics are used to sample temperature (T) and pressure (P), with only a different ROM necessary to acquire and process the data for Argos transmission.

The temperature probe is manufactured from a stainless steel tube, 10 cm long, and 0.5 cm outer diameter. The probe contains a thermistor packed in thermally-conductive grease. Time response was measured by plunging the probe from room temperature into a stirred, cold-water bath. The stirring rate was similar to ALACE's ascent rate, although flow direction was perpendicular to the probe's long-axis, rather than parallel, as would be during ascent. Results indicate a probe e-folding time response of 3.6 s. Assuming independent samples after 5 e-folding periods, and ALACE's ascent rate of 10-15 cm/s, independent temperatures are obtained over 2-3 m vertical scales.

PT-ALACE measures T and P every 3.2 seconds while profiling. The 8-bit a/d on the ALACE cpu (68HC11) is used to sample T and P, yielding typical resolutions of 0.08°C and 4 m respectively. By averaging over 4 m depth (1 LSB of P), T is measured on order 8-10 times. This oversampling is used to help increase the resolution of T, with the equivalent of 0.02°C /LSB (two extra bits) transmitted through Argos. T is averaged at the 4 m a/d resolution for shallow depths, increasing to 8 m bins for deeper values. The number of larger bins is chosen such that the profile will fit into the allotted number of Argos messages.

PT-ALACE spends 24 hrs on the surface transmitting to Argos before descending again for its next cycle. Multiple 32-byte Argos messages are used, with one transmitted typically every 90 s. A rotating buffer approach is utilized, where after each transmission the queue is rotated, pointing to the next message (cf. Sherman, 1992). Generally, temperature profilers use 2-3 messages, yielding 56-84 values of T. The 8 least significant bits of T are sent (2 highest bits thrown away), causing T to be ambiguous to multiples of 5.1°C. The full 10 bits are sent for the beginning data bin in each message, thus removing initial T ambiguity. The rest of the T profile is then processed to ensure no large discontinuities. To date, over 40 PT-ALACEs have been deployed world-wide.

Is the present 0.02°C resolution good enough? Let the measured temperature T be defined as: $T(z,t) = \overline{T}(z) + dT + \delta$, where $\overline{T}$ is the 'mean' profile in depth z, dT is the natural variability, and δ is the instrument resolution. As long as $\delta << dT$, then it can be considered that the field is well-resolved. Any averaging performed to estimate $\overline{T}$ will be constrained by dT, not δ. Allowable values of δ are dependent upon locale: Upper ocean, with high variability, will not require a small δ, whereas deeper, quieter regions will.

Consider the variability due to internal waves, where vertical displacement η will result in a rms signal of $dT(z) = \eta \overline{T}_z$ ($\overline{T}_z = d\overline{T}/dz$). For a Vaisala frequency N (cph), the Garrett-Munk model (Munk, 1981) predicts $\eta = 7(N_o/N)^{1/2}$ m, with $N_o = 3$ cph. Assume N can be approximated by: $N^2 = g\alpha \overline{T}_z$, where g is the local acceleration of gravity, and α is the thermal expansion coefficient (that is, assume N mainly depends upon the local temperature gradient). Combining this with the GM model and $dT = \eta \overline{T}_z$ results in $dT = A \overline{T}_z^{3/4}$, where $A = 12.1(g\alpha)^{-1/4}$ is only weakly dependent upon T. For the main

thermocline ($\overline{T}_z \sim 0.02$°C/m), expected rms variability is dT ~ 0.14°C. If the intent of the profile is to estimate $\overline{T}(z)$, then knowing T to within 0.02°C is more than adequate.

The amount of depth averaging, Δz, to perform should be chosen such that expected temperature differences exceed the instrument resolution. If T is averaged over Δz, then change in T between bins will be $dT \sim \Delta z \overline{T}_z$. Value of Δz is selected so dT exceeds δ, or equivalently: $\Delta z > \delta / \overline{T}_z$ (i.e. if $\overline{T}_z$=0.02°C/m, and δ=0.02°C, then 5 m averages of T (dT~0.1°C) should appear relatively smooth).

As ALACE rises, its ascent rate is modulated by the local vertical velocity of the internal wave field. Since internal wave vertical velocities are small compared to ALACE's ascent rate (order 1-2 cm/s compared to 10-15 cm/s) they should not significantly alter flow rate past the temperature probe. Thus the time response of the sensor should not be significantly affected by the local internal wave field. Furthermore, ALACE's ascent velocity is determined by the balance of buoyancy and drag: $B = C_d w^2$, where B is the buoyancy of the instrument, C_d is a drag coefficient, and w is the vertical velocity relative to the local water. As long as B is constant, w should also be constant. Therefore, although ALACE's ascent rate is modulated by internal waves, local flow past ALACE should remain relatively constant (ALACE is just moving up and down with the local volume of water).

Examples of temperature variability are 76 T profiles taken within 40 km and 10 days of each other in May 1992 by LAMP, which provides millidegree and centimeter resolution (see Section 4). Fig. 1 shows that instantaneous profiles have vertical displacements as large as 25 m. Note for the typical 10-25 days between profiles for a PT-ALACE, only one of the profiles in Fig. 1 would be collected, and thus be available to say something about the local hydrography. From a single profile, measured T(z) may be as much as 0.5°C away from the mean, even at 300 m depth. In this case, T(z) resolved to only 0.05°C would provide a well-defined profile within the natural variance of the field. This data set is atypical, with rms vertical displacements of order 10 m for N=2.5 cph, while Garrett-Munk's model predicts 7-8 m rms displacement. The more energetic internal wave field results in higher natural variability, and a lower requirement for instrument resolution.

As a comparison with the PT-ALACE, typical XBT (expendable bathythermograph) performance exhibit standard deviation errors of 0.05°C between probes, with errors up to 0.16°C (Roemmich and Cornuelle, 1987). Additionally, Roemmich and Cornuelle performed a plunge test of an XBT into a strongly stirred bath and found an 8-10 minute time constant. Many investigators have also found a discrepancy between true fall rate and Sippican's depth-time equation, resulting in 26 m offset at 750 m depth (Hanawa and Yasuda, 1992). Heinmiller et al.(1983) report a random error in fall rate between probes, resulting in O(10 m) errors. The PT-ALACE thermistors are calibrated at a minimum of 5 points (5-30°C), with standard deviation errors of <0.003°C. The type of thermistor used (manufactured by YSI) has a reported typical drift rate of <0.02°C over an 8 year span. The biggest concern in accuracy is due to the 8-bit a/d being over-resolved by 2 extra bits to obtain δ=0.02°C, thus accentuating non-linearity, thermal and temporal drifts of the a/d (one a/d LSB = 0.08°C). The ALACE uses a Paine pressure sensor, with specified repeatability within +/-4 m. Thus the PT-ALACE compares

favorably in both depth and temperature performance to a standard XBT.

General observation of the PT-ALACE data suggest that δ=0.02°C results in well-defined, smooth profiles. However, deeper instruments may require better resolution. An increase to δ=0.01°C can be transmitted in the same number of bytes, as the resultant 2.56°C ambiguity is still easily identified within profiles (as is done with the CTD-ALACE, see below). A better a/d converter would improve the overall accuracy of T, which is presently constrained to the 8-bit a/d resolution.

3. CTD-ALACE

The next modification to the PT-ALACE is the addition of an inductive-type conductivity sensor, manufactured by Falmouth Scientific, Inc. (FSI). The conductivity sensor is mounted next to the temperature probe, with the electronics located inside ALACE. The sensor geometry is shown in Fig. 2. Two toroidal coils (a 'drive' and a 'sense' coil) are contained within the 2.3 cm ID x 4.6 cm OD housing. The two coils are coupled by the sea water path, which provides a single loop path of resistance R (dependent upon the conductivity of the water). The sense coil output is proportional to the sea water conductivity (Fougere et al. 1992).

Errors in conductivity can occur due to fouling from biota passing through, or lodging in, the conductivity cell. The magnitude of the error is roughly proportional to the fraction of the cell volume that is fouled. The large volume of the inductive-type cell makes it less susceptible to fouling from individual biota than the smaller electrode-type conductivity sensors. Additionally, the large volume allows better flushing at ALACE's slow ascent rates. The inductive cell has the further advantage that there is no electrode degradation problem for long-term deployments. However, other long-term effects are an issue (i.e. stability of sensor core windings, magnetics, and electronics). Early versions of the FSI sensor employed an anodized aluminum housing, which have exhibited corrosion problems (quite severe in some ship-board systems). The first CTD-ALACE, deployed in Feb. 1992, was outfitted with this early version, and has shown degradation (see below). FSI has since gone to ceramic housings, and has reported that the corrosion problem has been solved.

A small 4 electrode conductivity cell (manufactured by Ocean Sensors, Inc) was also investigated. Although this cell has good low-flow flushing characteristics, its small cell volume makes it very susceptible to spurious reading due to biota/detritus entering, and sometimes lodging in the sample volume.

The time response of the FSI conductivity sensor is controlled mainly by the flushing time of the volume. Boundary layers are small compared to total cell volume, therefore conductivity is fairly insensitive to side-wall temperature anomalies (Lueck 1990, Fougere et al. 1992). If the sensor dynamics is modeled as a 10 cm/s flow at the entrance of a 2.3 cm dia tube of 5 cm length, 98% of the cell volume should be flushed in at least 1 s, or 10 cm (Appendix). To minimize sensor mismatch in time response, a smaller temperature probe is used (3.2 mm outside diameter), with an e-folding period of 1.6 s. This may still result in T lagging C by order 0.2 m (Appendix).

To increase instrument resolution over that available in the PT-ALACE, an additional electronics card has been added which includes a 12-bit a/d, used for both

pressure and temperature sensors. T and P resolution is increased to .005°C and 0.25 m respectively. The FSI electronics output conductivity (C) as a function of frequency, which is measured by the ALACE CPU to the equivalent of 0.001 mmho/cm resolution.

Since the majority of the conductivity response is due to temperature, and thus represents redundant information, it is optimal to remove this signal before transmitting the data. Ideally, this would be done by computing salinity (S). ALACE's limited ROM size does not accommodate the additional code required for the salinity equation of state, including the necessary floating-point routines. Therefore, S is not calculated directly. Instead, most of the temperature signal is removed from conductivity by using a simplified quadratic equation based on the equation of state. Let C' equal the corrected conductivity, defined by the quadratic: $C' = a_0 + a_1T + a_2T^2 + b_1C + b_2C^2 + cz$, where all a's, b's and c are constants. Values of the constants are determined by performing a singular-value-decomposition (SVD) on the above quadratic, using S(T,C,z) from the true equation of state for the desired value of C'. That is, the matrix below of n (=200) equations is solved using SVD to obtain the optimum values of the constants.

$$\begin{bmatrix} 1 & T_1 & T_1^2 & C_1 & C_1^2 & Z_1 \\ 1 & T_2 & T_2^2 & C_2 & C_2^2 & Z_2 \\ 1 & T_3 & T_3^2 & C_3 & C_3^2 & Z_3 \\ .. & .. & .. & .. & .. & .. \\ 1 & T_n & T_n^2 & C_n & C_n^2 & Z_n \end{bmatrix} \begin{bmatrix} a_0 \\ a_1 \\ a_2 \\ b_1 \\ b_2 \\ c \end{bmatrix} = \begin{matrix} S_1 \\ S_2 \\ S_3 \\ .. \\ S_n \end{matrix}$$

Ranges used for S, T, and z are 33-36 PSU, 5-30°C, and 0-1000 dBars respectively, thus matching expected ranges of the CTD-ALACE (C is determined from the equations of state using S, T, and z). The constants from the SVD are then programmed into the CTD-ALACE to allow computation of C'. Differences in using this simplified quadratic as compared to the true salinity range from +/-0.15 PSU. These small differences signify most of the dynamic range of C (i.e. from 40-70 mmho/cm) has been reduced to the equivalent of true salinity (33-36 PSU).

To recover S, the transmitted value of C', T, and z are used in post-processing to invert the quadratic, yielding the original conductivity value. The values of C, T and z are then used in the equation of state to estimate S. This process allows C to be transmitted using 1/8 of the dynamic range required for T.

The CTD-ALACE was developed primarily to measure sound speed c, estimated by using the derived equations relating (S,T,P) to c (i.e. the Chen and Millero equation or the Del Grosso equation). These equations are usually considered to be accurate to 0.25 m/s. Recent acoustic tomography measurements by Dushaw et al.(1993) suggest Del Grosso's equation is accurate to 0.1 m/s to 4000 m, while Chen and Millero's equation is good to 0.5 m/s. Oceanographic instruments which measure sound speed directly (using short-path acoustic travel time) are also generally quoted with 0.25 m/s accuracy (i.e. Applied Microsystems Ltd. SVP-16). Therefore, using a CTD to measure sound speed yields equivalent accuracy as direct methods, while also providing useful hydrographic data. To

obtain 0.25 m/s resolution for general values of T, S in the upper 1 km of ocean, T must be resolved to 0.06°C, and S to 0.15 PSU. Presently, transmitted T and S are resolved to 0.01°C and 0.02 PSU, resolving c to better than 0.05 m/s.

One CTD-ALACE has been deployed in the Central North Atlantic. A profile is performed every 10 days, with the first one taken in Feb. 1992. The instrument's drift track for the first 25 profiles is shown in Fig. 3. Each profile's data are transmitted in four 32-byte Argos messages over a 30 hr period, corresponding to 68 S, T samples in depth. Depth resolution is 5 m from 0-220 m, and 10 m from 220-460 m. Transmitted T and S resolutions are .01°C and .02 PSU respectively. The instrument's neutral depth is 500 m.

Dr. W. Jenkins (WHOI) performed a series of CTD stations on year-day 277 from the RRS Darwin (Fig. 3, dashed line). The timing placed these stations 4 days later than CTD-ALACE profile 22, and 6 days before profile 23. The location of Darwin station 7 was chosen to sample close to the same water column in which ALACE was drifting. Fig. 4 shows the associated T profiles. Note the nearly isothermal layer between 170-210 m depth in Darwin 7. This layer is not seen in either Darwin 6 or 8, and so is localized North-South to less than 100 km. CTD-ALACE 22 shows some of this feature (remember, separated by 10 km and 4 days time), while profile 23 shows perhaps a slight remnant. Fig. 4 indicates ALACE's T agrees to within the natural variability seen in the CTD's stations. From comparison within the isothermal region, ALACE T appears to be within 0.02°C of the CTD cast. It is not known how much natural variability exists within this layer, and therefore if the observed offset is due to instrument or ocean.

Unfortunately, the conductivity cell suffers major offsets beginning at profile 19. If the average deep S value (300-470 m) is adjusted to fit the mean T-S curve as estimated from Levitus, the resulting match to the Darwin stations is fair for T<18°C (Fig. 5) The good match between Darwin and ALACE at 14°C has not been forced, but is the result that the Darwin T-S curve also agrees with Levitus. There is greater variability above 18°C, with ALACE 23 showing a much fresher upper thermocline (T>20°C) than the others. Accuracy of the CTD S(z) depends greatly on how much true natural variability there is. Deep values (T <16°C) suggest S(z) is within 0.04 PSU of the Darwin values. Observations by researchers in the same area (Jenkins 1992, Rudnick 1992) show natural variance in the T-S curve of less than 0.02 PSU for T <14°C, increasing to 0.06 PSU at 16°C. Given the CTD-ALACE S resolution is only 0.02 PSU, deep values suggest that the FSI sensor is accurate to 0.02-0.04 PSU.

Variability in the ALACE T-S curve for 18°C<T<22°C (Fig. 5) occurs at the maximum temperature gradient (Fig. 4), perhaps indicating an effect of the of time response mismatch of the C and T sensors. Note S is fresher (i.e. measured C is less than expected, or alternatively T is warmer) than Dr. Jenkin's values, and that the CTD-ALACE measures while ascending (moving from cold to warm water). This suggests that if there is a problem, C is lagging T, and that FSI cell's thermal mass is important (see Appendix). ALACE T profiles were adjusted using various depth lag values in an attempt to match ALACE salinity with Jenkin's. However, no lag resulted in enhanced performance. An example of why this was so is seen in ALACE profile 22, where S compares well with Jenkins' between 20°C<T<22°C, which is still very much in the maximum temperature gradient. Thus no adjustment is required for this section, and any attempt only results in a

worse fit. It appears that the upper water variability is either real, or an artifact of a sensor failure which causes greater errors at low pressure than at greater depth.

Long-term salinity drift was investigated by computing mean T-S values between 300-470 m for the CTD-ALACE and comparing these with the associated Levitus T-S curves for the same location as ALACE (to within 0.5 degree of latitude and longitude). Levitus seasonal values were interpolated to the ALACE's profile date (Fig. 6). Differences (Fig. 7) are due to either natural variability or instrument error. The first profile agrees within 0.02 PSU with Levitus. This is followed by an abrupt 0.06 PSU jump for profile 2, and then what appears as a long-term linear drift equivalent to .04 PSU/month. Beginning at profile 19, the sensor begins to degrade rapidly. Resultant errors in sound speed c caused by the drift in S (Fig. 7) are +/- 0.1 m/s over the first 18 profiles, increasing up to 1 m/s for the last profile. Although these shifts in S are quite significant for hydrographic work, for the first 18 profiles they are of the same order accuracy as the sound speed equation.

To assess the expected natural variability, one can look at differences within the Levitus data set. Variance arises from spatial and temporal changes. Both are investigated by extracting Levitus values for all four seasons at the CTD-ALACE's profile locations. An envelope of T-S curves is computed using profiles from all seasons (hence ignoring date of profile). This envelope represents the expected annual variability. Additionally, an envelope is calculated by using the T-S values that have been interpolated in time to date of profile (as used in Fig. 7). This envelope estimates the seasonal variability. For T<15°C, variance in seasonal and annual Levitus T-S curves are 0.02 and 0.1 PSU respectively (Fig. 8). Thus, if time of year is ignored, half the drift in Fig. 7 could be explained by annual variance. Assuming seasonal T-S adjustments are correct, only 10% of the observed drift in Fig. 7 can be justified by natural variability.

Besides long-term instrument drift, there is the question of accuracy of S within each individual profile. By using offsets in Fig. 7 to remove drift, the resultant T-S curves are forced to agree with the seasonal Levitus values for T<14°C (Fig. 8, only the first 18 profiles are plotted, avoiding the drastic offsets in the later profiles). Note that for T<14°C the spread in measured S is 0.02 PSU, which corresponds to the resolution of the CTD-ALACE, and to the expected variability in seasonal Levitus T-S values. Measured variability of S as a function of T seems to agree with Levitus fairly well. There are 4 points where salinity is fresher than predicted by the annual Levitus values. These are warm-water, near-surface values, where observations are most likely to be influenced by bubbles/biota contaminating the conductivity reading.

Salinity variance from the average Levitus T-S curve leads to a corresponding deviation in sound speed. The Levitus T-S (seasonal, annual) envelope values from above are used to calculate the maximum deviation of c. The resulting variances (Fig. 8) are less than (0.05, 0.10) m/s for T<16°C, increasing to (0.15, 0.35) m/s for T>18°C. Deviations of the CTD-ALACE salinity from the average Levitus T-S (Fig. 8) lead to sound speed variances of 0.1 m/s for T<16°C, increasing to 0.25 m/s for T>18°C. The four anomalous, near-surface salinity values mentioned above result in ~0.5 m/s difference in c. These results simply re-emphasize that sound speed does not depend strongly on salinity. The deviations in c due to S can be compared with the natural variability of sound speed

profiles (Fig. 9, using S values corrected to Levitus, as in Fig. 8). Here, 98% of the variance in sound speed is due to T, and 2% from S. For this locale, the uncertainty in c due to S is overwhelmed by the temperature signal.

Performance of the conductivity cell is a disappointment due to instrument drift problems (Fig. 7). There appears to be a long-term linear drift of 0.04 PSU/month, followed by a rather catastrophic failure causing offsets approaching 1 PSU. Such behavior may result from the FSI anodized head corroding over time, thus changing the geometry/sensitivity of the cell, perhaps followed by a salt-water leak through the wall, causing severe offsets. The initial offset between profile 1 and 2 of 0.06 PSU is also troubling. This corresponds to ALACE being in the water (at 500 m) for 10 to 20 days respectively. Mechanisms acting on these time scales to cause such an offset are presently not clear. One would expect corrosion of the conductivity head to cause drift in one direction, as observed later on. One possible explanation is that the ALACE pressure case (6061 aluminum, unanodized) formed a passivation layer over the first 10-20 days, thus altering the far-field of the conductivity sensor, and lowering the measured conductivity. Comparison with Dr. Jenkin's CTD values below 18°C suggests accuracy within a profile of 0.04 PSU (Fig. 5). This may be affected to some extent by the large offsets observed in S (Fig. 6) leading to noisier salinity profiles. Comparison of the first 18 profiles (Fig. 8) suggest S variance of 0.02 PSU (equal to instrument resolution) for deep values.

The FSI conductivity cell observed drift rate of 0.04 PSU/month greatly exceeds FSI's quoted stability of 0.001 mmho/month (equivalent to ~ 0.001 PSU/month). FSI confirmed that the poor performance is most likely due to the anodized head corroding (personal communication). It is their belief that the new ceramic head design has solved this problem.

4. LAMP

The time duration of microstructure data sets has generally been confined by the scientist's tolerance for staying at sea and the funding agent's ability to pay for ship time. By perhaps mutual agreement (??) this seems to reach a maximum period of about 1 month. Microstructure data sets spanning a long time period have been lacking. This leaves a void in understanding the climatic variability of dissipation (although multiple stations over many years near the same site has provided some insight, i.e. with equatorial experiments). The LAMP (Long-term ALACE Micro-temperature Profiler) is an effort to alleviate this problem.

The central elements of the LAMP are two micro-temperature probes and a 200 mb hard disk. By using two probes, a cross-check can be performed on sensor health, along with some analysis of horizontal correlation of microstructure (probes are separated horizontally by 18 cm). It also increases the odds of having at least one probe survive a long deployment. Data is recorded while the instrument is descending. Normal descent rate during data acquisition is 5-8 cm/s. After a set number of cycles, LAMP remains on the surface, transmitting to the Argos satellite system. The instrument is recovered by using the location provided from Argos (~1 km accuracy), followed by a shipboard direction finder tuned to the Argos frequency.

The temperature probes and front-end electronics are manufactured by Sea-Bird

Electronics (SBE). The temperature probe consists of a fast time-response thermistor (FP07). Its output is high-pass filtered on the SBE analog board, and then sampled by a 16-bit a/d. The a/d board is controlled by an Onset TattleTale 6 computer with 1 Mb memory. At the end of each profile the data is written to hard disk. To supply the extra power required, three lithium 30 A-h, 15 volt battery packs are used in parallel (compared to the 2 packs normally used in ALACE). In case of a malfunction causing low battery voltage, the instrument goes into a low-power state for the remainder of the deployment, and then switches in a spare battery pack for final pumping of the bladder plus Argos transmission. The spare battery should allow for 90 days of Argos transmission at the end of deployment. To accommodate the added electronics and batteries, the standard ALACE pressure case has been stretched .3 m to a total length of 1.24 m and a mass of 30 Kg.

In May 1992, LAMP was deployed for a 10 day period in the mid North Atlantic (26°N, 28°W) in conjunction with the North Atlantic Tracer Release Experiment (NATRE). LAMP cycled every 3 hours, collecting 76 profiles with an average depth of 350 m (Fig. 1). On recovery, one probe had some bio-fouling at the base of the thermistor. Inspection of dT/dz variance levels between probes, averaged for depths>200 m for each profile, shows that after profile 26, variance of sensor 2 falls to 65% of sensor 1's value (Fig. 10). Frequency spectra for both probes are averaged over z>200 m for each profile, with spectra compared before and after profile 26. The change in response of sensor 2, as compared to sensor 1, is similar to a single-pole filter with a -3 dB point at 8 Hz (Fig. 11). If the attenuation was due to a uniform layer of contaminant, its thickness would be $L = (kt)^{1/2} = (k/(2\pi f))^{1/2}$, where k is the contaminant thermal diffusivity and f is the e-folding frequency. Taking k equal to that of water and f=8 Hz, yields thickness L of order 0.05 mm. Fouling by such a small thickness seems reasonable. This indicates the advantage of recording two probes, and the potential problem of both probes fouling over a long-term deployment.

Distribution of dT/dz variance based on 0.5 m averages is close to log-normal, with standard deviation of $\ln(dT/dz)^2$ equal to σ=1.9. Baker and Gibson(1987) proposed a model for estimating confidence limits for log-normal distributions. Using their model and the above value of σ=1.9, 95% confidence limits can be be placed on the profile-averaged values in Fig. 10 (each profile average consists of ~300 0.5 m estimates). Variance between consecutive profiles seems to be well represented by these confidence limits. High variance in profile 18 is due to a strong mixing event over a 7 m interval. The decrease in variance during the second half of the deployment is statistically significant. It is either an indication that the dissipation rate has decreased, or that the probe response is slower. Given that both probes track each other, further fouling would require both probes to have been fouled at the same time to the same degree, and thus seems unlikely. The lower variance is most probably due to lower dissipation rates.

dT/dz spectra have been computed over 2 m scales (2048 data points Fourier transformed, spectral densities averaged over 16 successive frequency bins). For each profile, the minimum, maximum, and average spectral density values are calculated for z>200 m (where the background temperature gradient is constant to within a factor of 2, see Fig. 1). Thus the minimum and maximum curves form the lower and upper boundaries for all spectra for that profile. These values are further averaged over the 76 profiles (Fig. 12). These profile-averaged minimum and maximum curves represent the envelope in

which all spectra lie between for a typical profile. They are displayed here to give an idea of expected spectral variability in any one profile.

The minimum and maximum values for all spectra for all profiles are also computed (Fig. 12). These all-inclusive minimum and maximum curves form an envelope in which all spectra lie between (i.e. they form the upper and lower boundaries for all spectra). Note the extreme variability, where at 5 cpm spectral values vary by as much as 5 orders of magnitude for the entire data set, with the typical maximum value 1000 times greater than the minimum within an individual profile. All spectra fall into the noise floor before reaching the Nyquist frequency of 30 Hz. The sharp spectral rolloff is due to both the dissipative nature of the ocean and the response of the thermistor, typically modeled as a double-pole filter (Gregg and Meagher 1980, Vachon and Lueck 1984).

The contribution of noise to dT/dz is removed by only integrating dT/dz spectra out to the noise floor. For each individual spectrum, it is necessary to determine when the spectrum falls into the noise. From the profile-averaged minimum spectrum, the shape of the noise floor is modeled (Fig. 12). The noise floor level is set to the expected upper limit. This is estimated by the value of the profile-averaged maximum spectrum at the highest frequencies (Fig. 12). Thus the modeled noise floor represents the upper bound of the measured noise. When an individual spectrum falls below this noise level, the remaining high frequency spectral values are set to zero. The lower frequencies are corrected for probe response, and the spectrum is integrated to give the estimate of $(dT/dz)^2$. Note no estimate of the noise floor is removed. The modeled noise floor is simply used to define when an individual spectrum is in the noise.

LAMP is currently deployed in the same area as the first NATRE cruise. It is programmed to perform 200 profiles, one every 1.22 days, for a 244 day total period (due at the surface again mid-June 1993). This data set should provide insight into the long-term variability of $(dT/dz)^2$.

5. Conclusions

ALACE provides a convenient platform for additional instrumentation. This paper describes three different types of instruments (temperature, CTD, and microtemperature) which exploit ALACE's profiling nature. Additionally, data can be collected while ALACE is at its neutral depth. Indeed, most ALACE's now return the average temperature and pressure at its neutral surface, using athermistor located inside the pressure case. Data sets which can be compacted to a small size (i.e. O(100) bytes) can be successfully transmitted through Argos in the 24 hour time duration when the instrument is on the surface. This removes the necessity of retrieving ALACE. When this is not possible, as with the microtemperature version, recovery of the instrument is necessary.

Due to ALACE's potential multi-year life-span, sensors must be stable with low-corrosion characteristics. As seen from the tested CTD-ALACE, this was not the case for the FSI anodized head conductivity cell (now no longer being manufactured). A large drift in salinity is observed (0.04 PSU/month), followed by extremely large offsets (approaching 1 PSU) after 6 months, where it is assumed that the head has corroded so severely that there is actually a leak path. FSI has manufactured a new ceramic head which reportedly solves the corrosion problems. Likewise, microtemperature measurements rely

upon fragile thermistors to obtain the required fast time response. The present 8 month deployment should provide insight into how well these sensors can actually survive at sea over a long time span.

ALACE supplies a remote data collection ability which is not biased by ship schedules or weather conditions. Argos transmissions have not been a problem, even from ALACEs in the Southern Ocean during winter. Cost of data is lowered by removing ship and personnel time. The ALACE platform does constrain measurements to be taken along the track of a Lagrangian drifter. This is beneficial if one wants to track properties within a specific water mass. Otherwise, multiple instruments are required.

Acknowledgments: The profiling instruments were developed by the Instrument Development Group under the direction of Dr. R. Davis. Efforts of J. Dufour, G. Pezzoli and L. Regier have greatly contributed to the instruments' successes. Dr. J. Ledwell graciously allowed deployment/recovery of LAMP as a last-minute addition during his NATRE May 1992 cruise. Dr. W. Jenkins altered his CTD station locations during the Oct. 1992 Darwin cruise to accommodate a station near the CTD-ALACE, and then made his CTD data readily available to us. Funding has been provided by ONR for the PT-ALACE and LAMP. The CTD-ALACE development was supported by the Oceanographic Support Block (PE 62435N PN 3585) at the Naval Research Laboratory, Stennis Space Center.

References

Baker, B. A. and C. H. Gibson, 1987: Sampling turbulence in the stratified ocean: Statistical consequences of strong intermittency. *J. Phys. Oceanogr.*, **17**, 1817-1836.

Davis, R. E., D. C. Webb. L. A. Regier, and J. Dufour, 1992: The autonomous lagrangian circulation explorer (ALACE). *J. Atmos. Oceanic Technol.*, **9**, 264-285.

Dushaw, B. D., P. F. Worcester, and B. D. Cornuelle, 1993: On equations for the speed of sound in seawater. *J. Acoust. Soc. Am..*, **93**, 255-275.

Fougere, A. J., N. L. Brown, and E. Hobart, 1992: Integrated CTD oceanographic data collection platform. *Oceanology 92 Conference,* Brighton, England, 26 pp.

Goldstein, 1965: *Modern Developments in Fluid Dynamics.* Dover Press, p. 297-309

Gregg, M. C. and T. B. Meagher, 1980: The dynamic response of glass-rod thermistors. *J. Geophys. Res.*, **85**, 2779-2786.

Hanawa, K., and T. Yasuda, 1992: New detection method for XBT depth error and relationship between the depth error and coefficients in the depth-time equation. *J. Ocean.*, **48**, 221-230.

Heinmiller R., C. Ebbesmeyer, B. Taft, D. Olson and O. Nikitin, 1983: Systematic errors in expendable bathythermograph. *Deep Sea Res.*, 30, 1185-1196.

Jenkins, W., 1992: Woods Hole Oceanographic Institute. Unpublished data from CTD stations during Darwin cruise 073, Oct 1992.

Lueck, R. G., 1989: Thermal inertia of conductivity cells: Theory. *J. Atmos. Oceanic Technol.*, **7**,???.

Munk, W. H., 1981: Internal waves and small scale processes. *Evolution of Physical Oceanography,* B Warren and C. Wunsch, Eds., The MIT Press, 264-291.

Roemmich, D.. and B.D. Cornuelle, 1986: Digization and calibration of the expendable bathythermograph. *Deep Sea Res.*, 34, 299-307.

Rudnick, D. L., 1992: University of Washington. SeaSoar survey of the Azores front, via personal communication.

Sherman, J., 1992: Observations of Argos Performance.*J. Atmos. Oceanic Technol.*, **9**, 323-328.

Vachon, J. and R. G. Lueck, 1984: A small combined temperature-conductivity probe. *1984 STD Conference and Workshop,* Marine Technology Society, p. 126-131.

Appendix

As with any CTD, it is imperative that measured values of C and T represent as closely as possible the same volume of water, such that salinity spikes are *minimized* (c.f. Lueck, 1990). A first-order approximation of the flushing-time for the FSI conductivity cell is given here. The FSI cell is modeled as a tube of length L=5 cm and radius a =1.15 cm (Fig. A1). Across the entrance is uniform flow U=10 cm/s. As the fluid progresses down the tube, a boundary layer of thickness δ forms. At a distance X, the flow will become fully developed (Poiseuille flow). This occurs at $X \sim 0.06a^2U/\nu$, where ν= kinematic viscosity (Goldstein, 1965). For U=10 cm/s, X ~80 cm. For the FSI sensor, the flow will never be fully developed. Boundary layer thickness δ, as a function of distance traveled down the tube, x, is given by (Goldstein, 1965):

$$\delta(x) = 1.72(\nu x/U)^{1/2} \ .$$

The velocity profile u(x,r) within the tube is taken as (let y=a-r = distance from wall):

$$u(x,r) = U_o \qquad \text{for } y>\delta(x),$$

$$u(x,r) = U_o\left[\frac{2y}{\delta} - \frac{y^2}{\delta^2}\right] \qquad \text{for } y<\delta(x),$$

where U_0 is chosen such that the mean velocity across the tube at any x is constant (obeying conservation of mass).

Assume a particle entering the tube at radial distance r also exits at r (effects of diffusion ignored). At time t=0, let there be a step change in salinity across the entrance of the tube. Let z(r,t) equal the distance down the tube that the step at radial distance r has traveled, where $z = \int u(x(t),r)dt$ is computed here by numerical integration. The volume V of the cell filled with the new S is directly computed from z: $V(t) = \int z(r,t)*2\pi r\, dr$ (Fig. A2). After 0.5 s the fluid not significantly influenced by the boundary layer has advected through the cell, accounting for 96% of the volume. The flushing rate then slows, with 98.5% flushed after 1 s, and 99.2% after 2 s. Diffusion will increase the last stages of the process by diffusing the old S out from the wall, into higher advection regions. However, given the small diffusivity for S (k~1e-4 cm^2/s), and the average value of δ = 0.08 cm, time to diffuse distance δ is $t = \delta^2/k \sim 60$ s, and help from diffusion is minimal. Considering only the above basic model, 96% of the volume should be flushed after the cell has moved one body length =L, with 98.5% flushed after 2L. This

should be valid for the range of CTD-ALACE ascent rates of 10-15 cm/s, where δ has not changed significantly.

The above analysis is flawed in that it assumes the inductive sensor field is constrained solely to the tube, with uniform field density. Furthermore, heat transfer between the cell wall and the boundary layer will contaminate the signal by warming/cooling the measured volume (c.f. Lueck, 1990). Self-heating on one hand is minimized by the small boundary layer. However, the cell body itself represents a thermal mass, which may provide a large temperature anomaly to the boundary layer, and therefore a larger error. Fougere et al.(1992) claim thermal mass is not a problem for their cell, although no specific numbers are given. The effect of self-heating during ascent would be for the cell to cool the water passing through, and thus lowering the measured conductivity.

Given a linear ramp in T, measured C will lag true C by approximately half its flushing time, corresponding to ~3 cm at 10-15 cm/s ascent rate of ALACE. The T probe can be modeled as a simple exponential response, with time constant τ = 1.6 s (measured in lab). For a linear ramp, it will lag true T by τ, equal to 16-24 cm for the CTD-ALACE ascent rate. The probe tip is located 3 cm above the entrance to the C cell. Therefore, given a constant dT/dz, measured T will lag C by 10-18 cm. At the top of the thermocline, where dT/dz may reach 0.25°C/m (i.e. Fig. 4), T may lag by as much as 0.05°C, leading to an overestimate of S of order 0.04 PSU. Post-processing can be used to adjust T upwards in depth by the estimated lag.

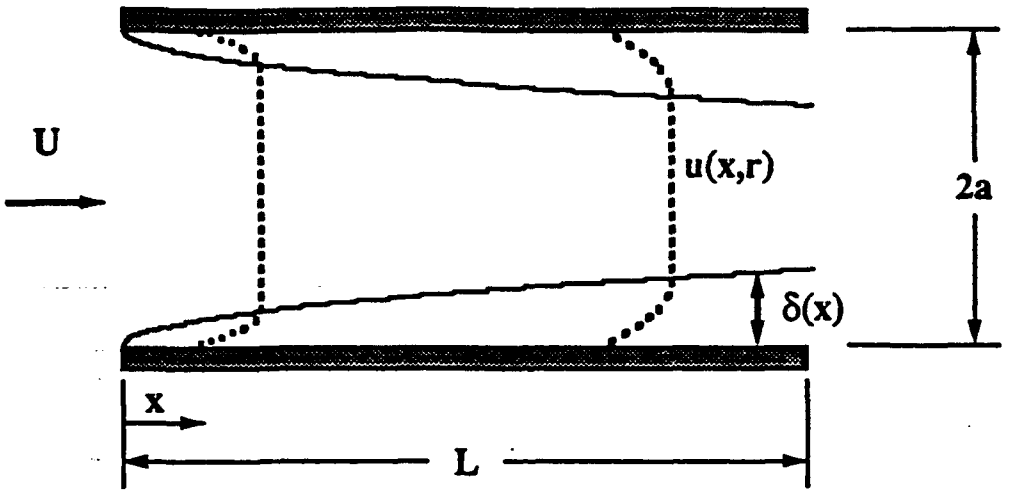

Fig. A1 Flow geometry for the FSI cell is modeled as flow through a tube of length L and radius a, with entrance velocity U. A boundary layer δ(x) forms along the wall, creating the velocity profile u(x,r). The above boundary layer has been accentuated, and is representative of U = 0.5 cm/s.

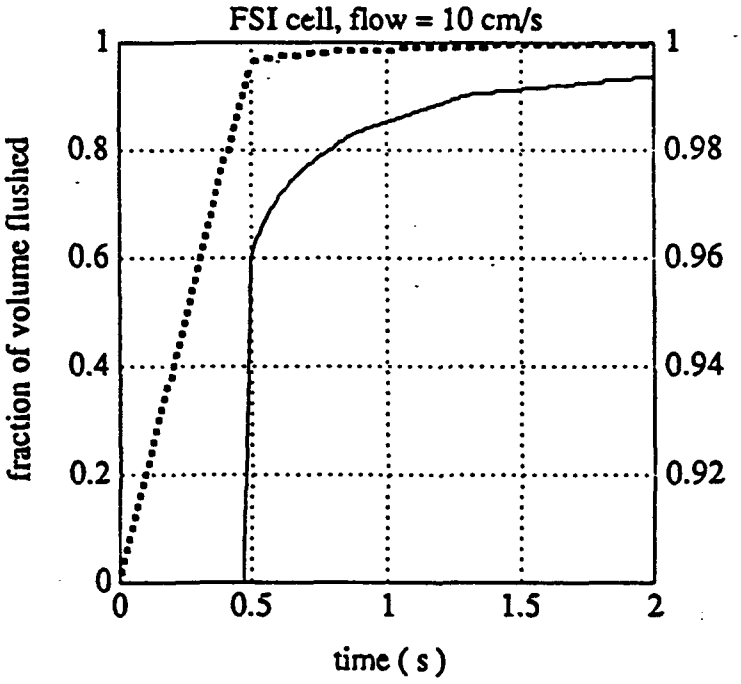

Fig. A2 Given a step response of S at the entrance of the cell at time t=0, the fraction of the cell volume with the new S is plotted above as a function of time. The dotted line scales with the left axis, while the solid line is the last 10% magnified, and scales with the right axis. Boundary layer significantly affects about 4% of the volume.

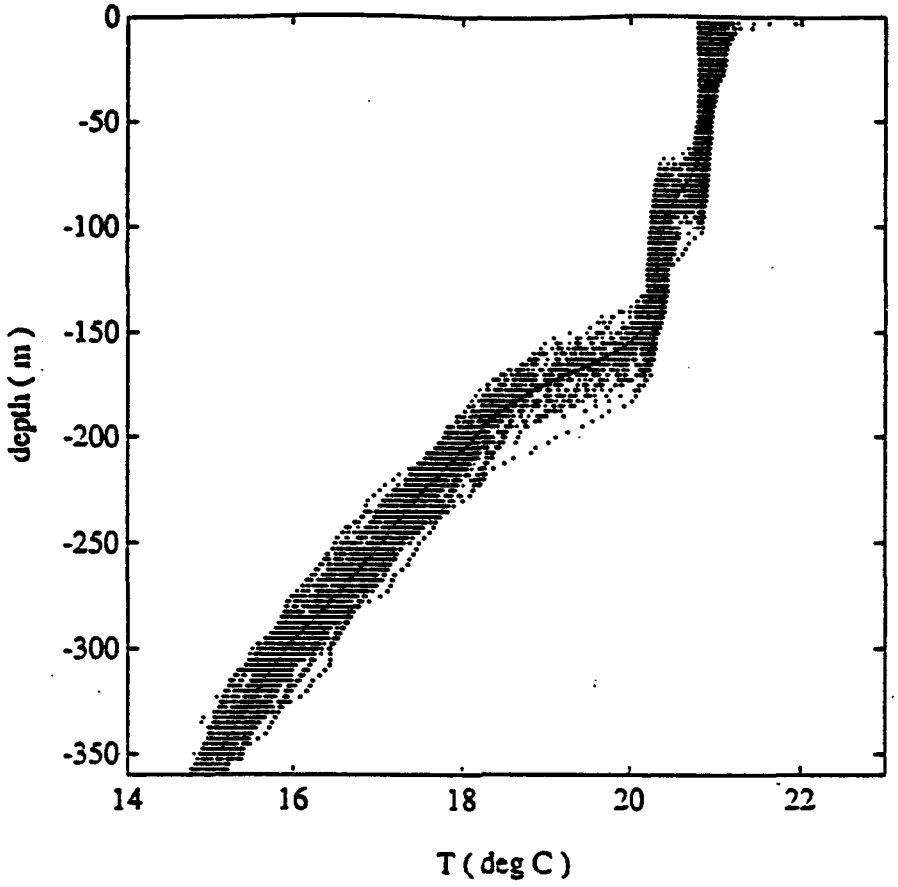

Fig. 1 Mean (solid line) and individual (dotted lines) profiles from LAMP deployment in May 1992. Each profile was taken 3 hours apart, with 76 total dives performed in 10 days. Temperatures are averaged into 2.5 m depth bins. Data set is marked by an energetic wave field, with rms vertical displacements of 10 m, compared to the GM internal wave model value of 7-8 m.

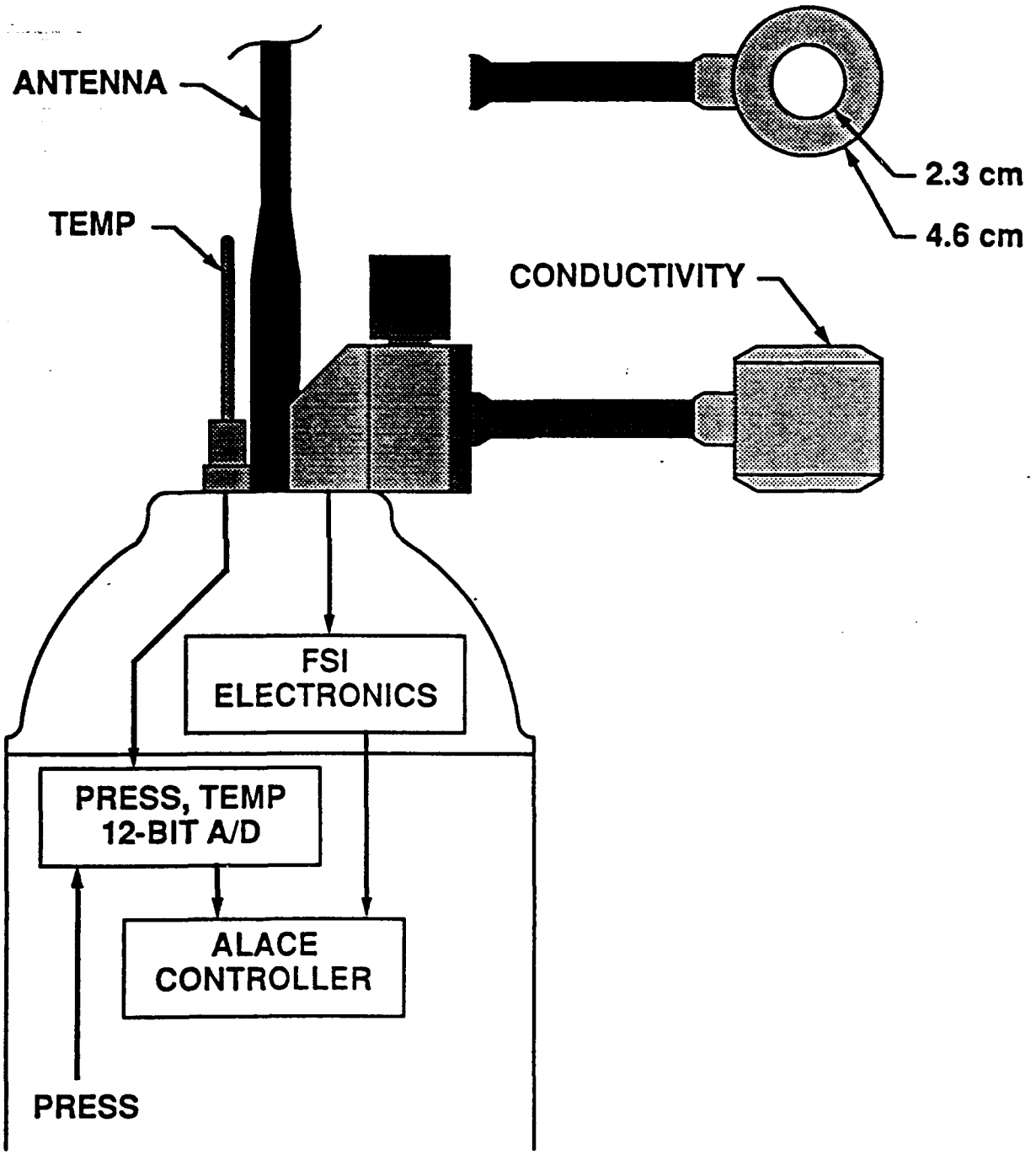

Fig. 2 The CTD-ALACE is modified by the addition of temperature sensor, conductivity cell (manufactured by FSI) and 12-bit a/d board. The FSI sensor is an inductive type, where 2 coils ('drive' and 'sense') located inside the sensor head are coupled by the sea water path.

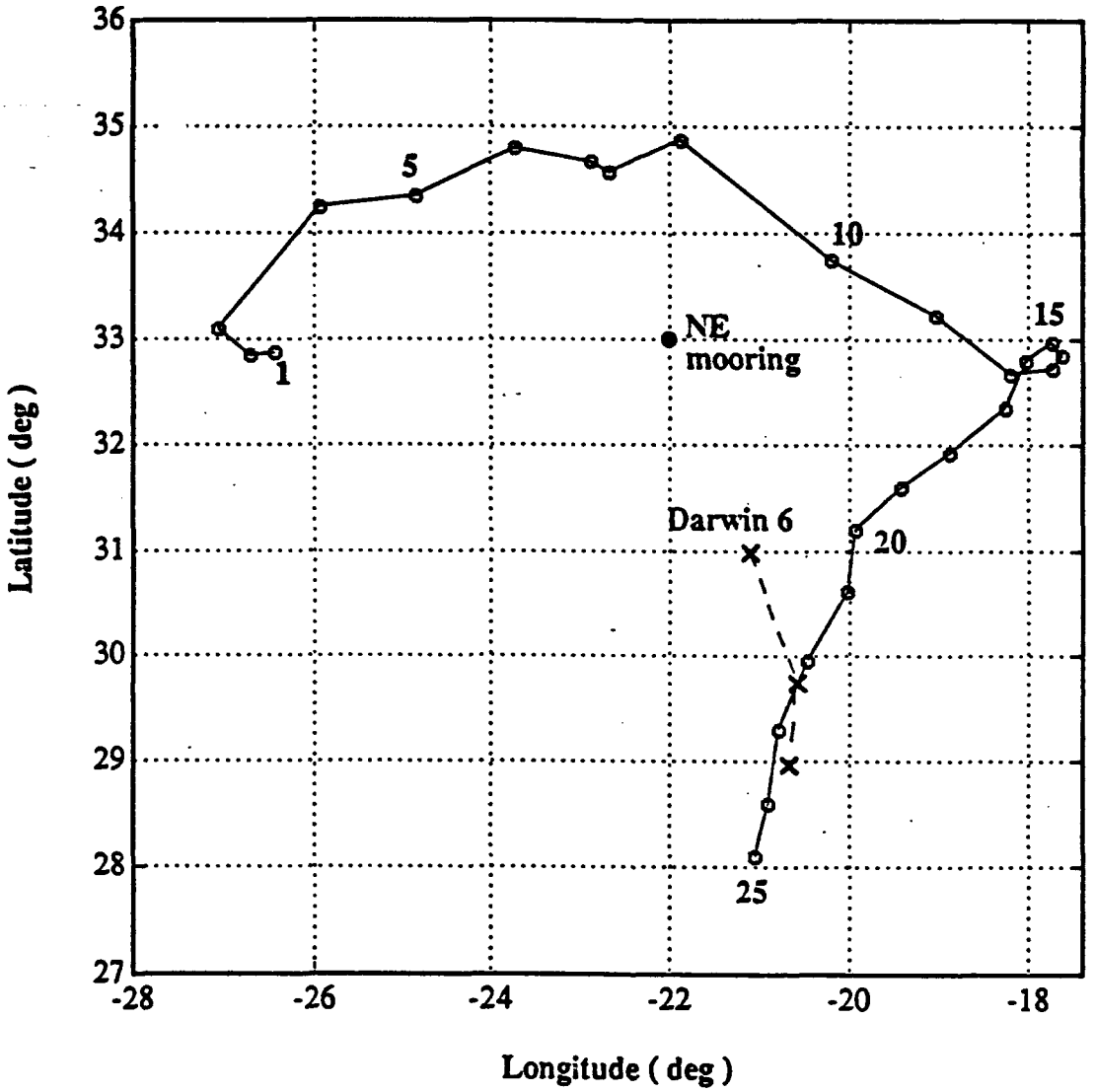

Fig. 3 The drift track of the CTD-ALACE (solid line) is marked at the location of each profile (every 10 days), with profile number noted on every fifth one. On year-day 277, Dr. Jenkins on the RRS Darwin performed CTD stations 6-8 (dashed line). Station 7, taken 4 days after ALACE profile 22, was situated to sample close to the same water mass as the CTD-ALACE. The Subduction NE mooring is also marked for reference.

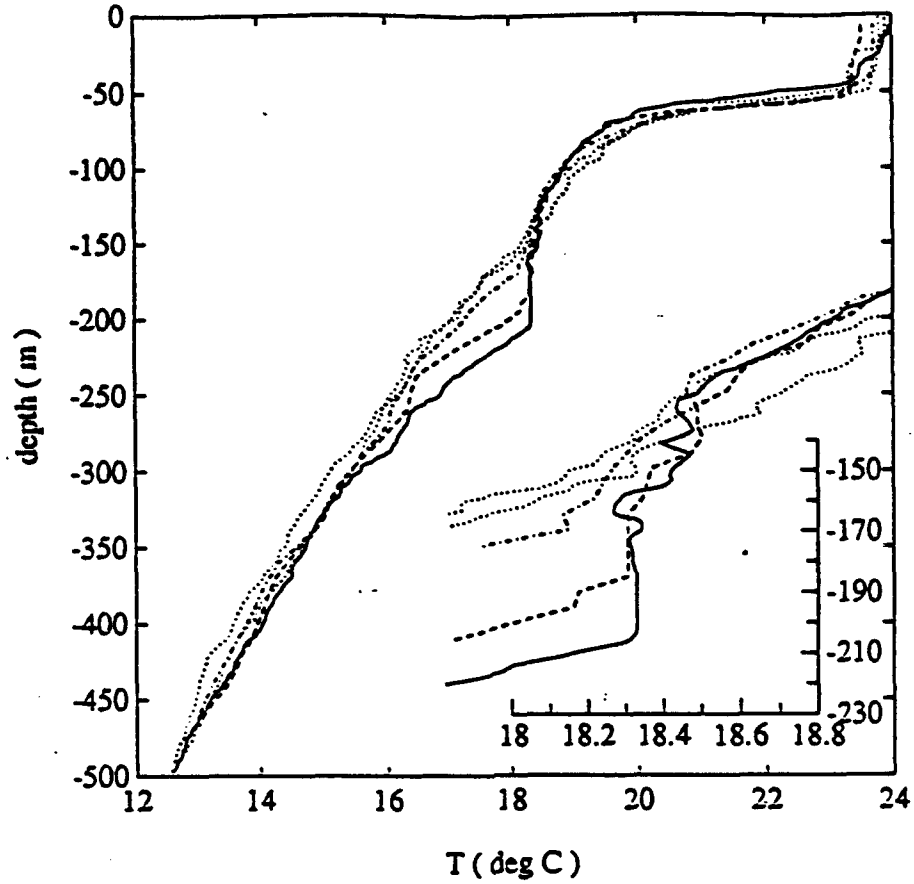

Fig. 4 Darwin station 7 (solid line) shows a nearly isothermal layer between 170-210 m, which is not present in stations 6 and 8 (dotted lines). ALACE profiles 22 (dashed) and 23 (dashed-dot) have similar T profiles to the Darwin CTD. A closer view of the isothermal region (inset) shows ALACE 22 is within 0.02 deg C of the Darwin value. It is not clear how much natural variability exists within this layer, and therefore if the observed offset is due to instrument or ocean.

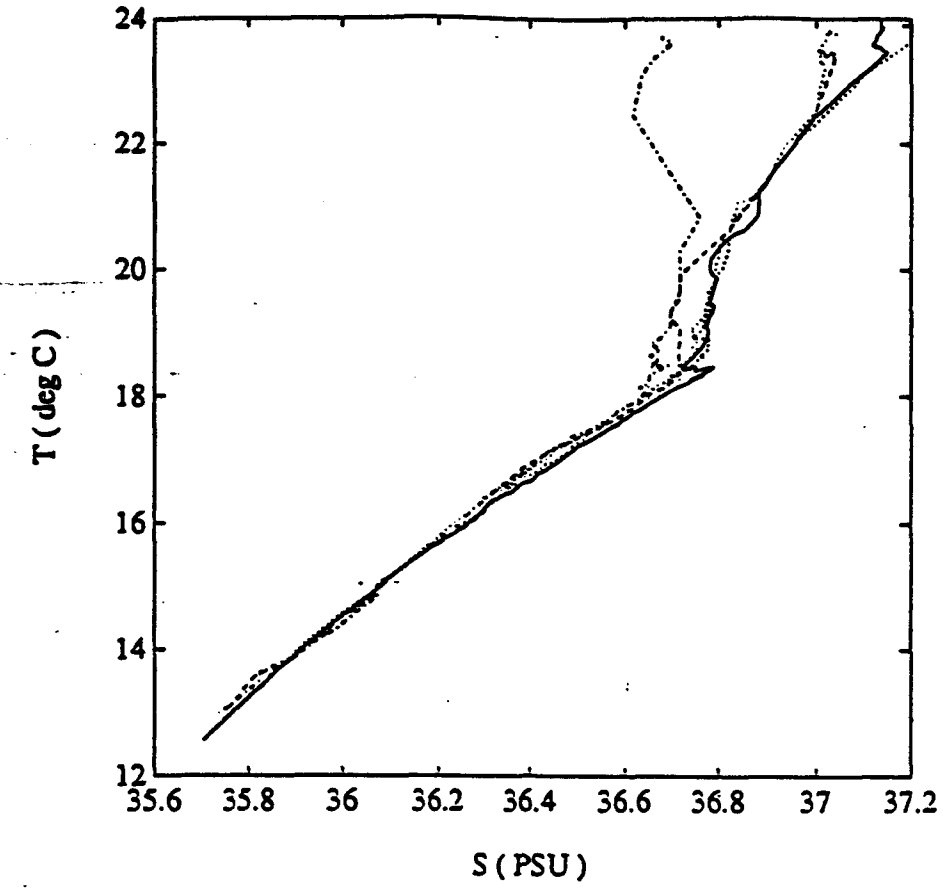

Fig. 5 T-S curves taken from Darwin stations 6-8 are compared to ALACE profiles 22 and 23 (line types correspond to Fig. 4). ALACE salinity values have been offset such that the average T, S values between 300-470 m fall on the Levitus T-S curve for the same locale and season. Agreement between ALACE and Darwin is therefore due to Darwin also agreeing with the Levitus values.

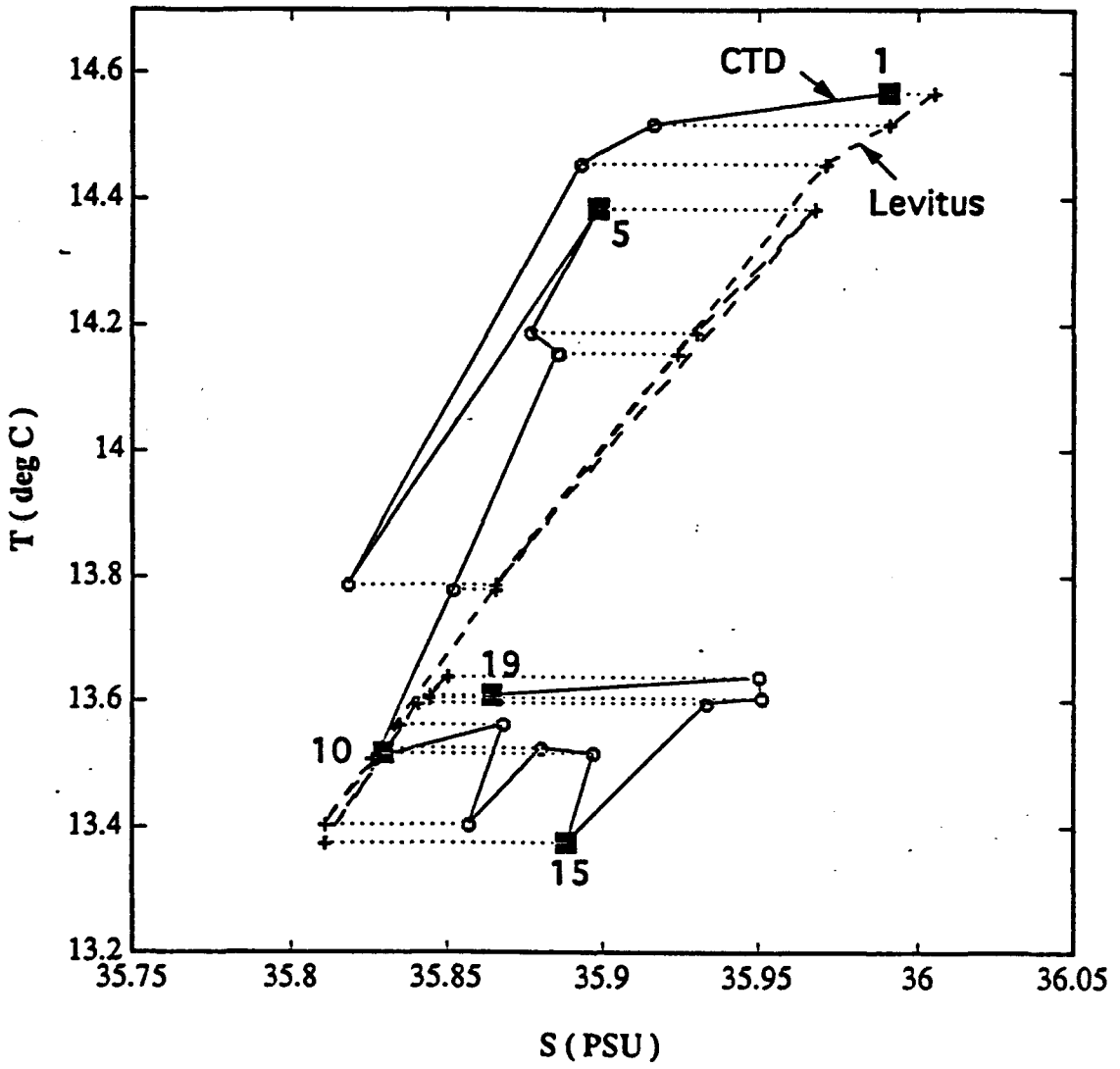

Fig. 6 Average T, S values are computed for each ALACE profile between 300-470 m (solid line, every 5th profile number noted). For the same location, Levitus T-S curves are interpolated between seasons to match ALACE's profile date. Using ALACE's mean T, the corresponding Levitus S is estimated (dashed lines). Salinity offsets between Levitus and ALACE are marked by the dotted lines.

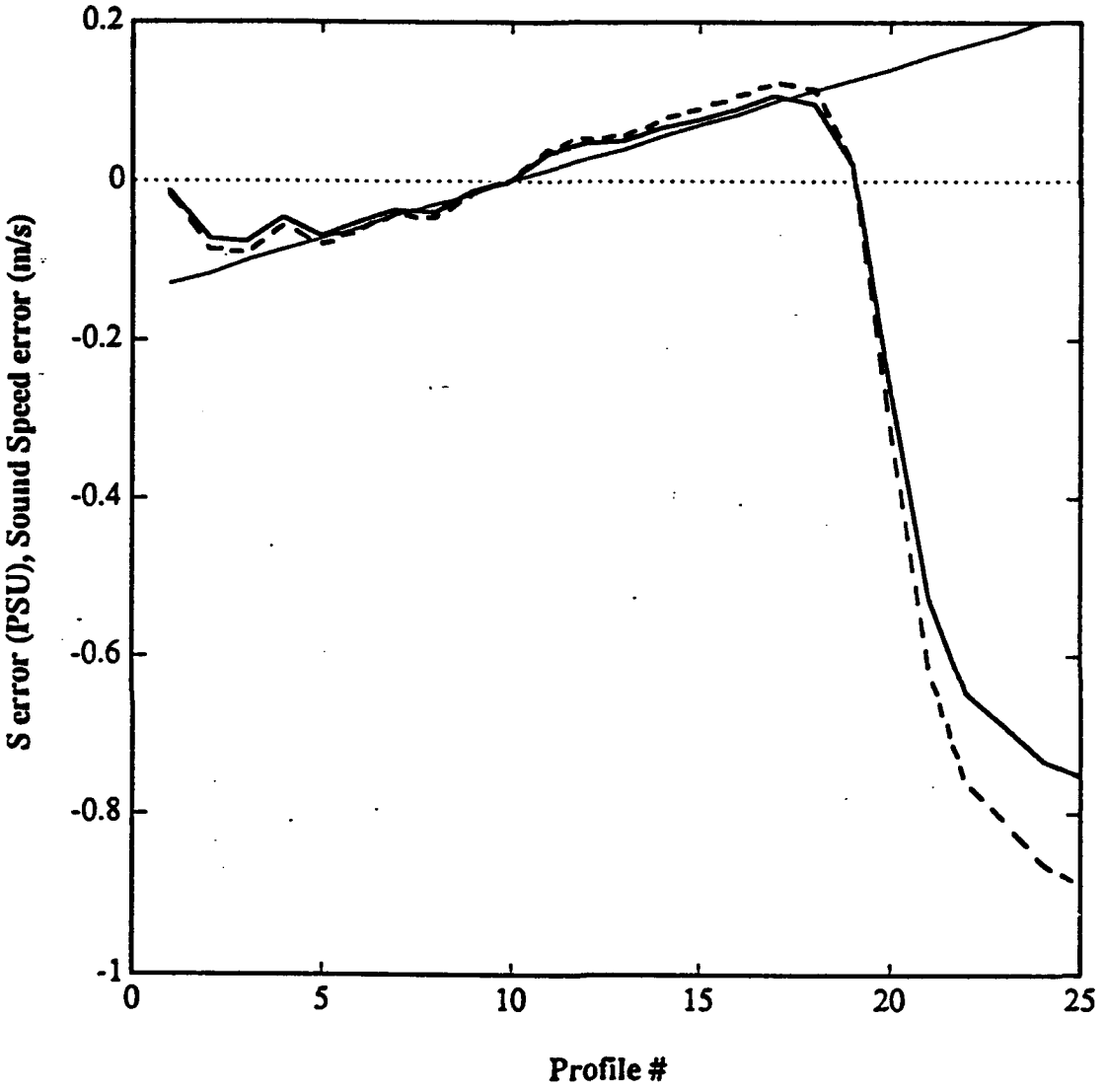

Fig. 7 From Fig. 6, ALACE S offsets are computed from the Levitus values, shown as a function of profile (each profile is separated by 10 days, solid line). If true T-S values are close to Levitus, then the above offsets can be viewed as instrument errors. There is a linear drift of 0.04 PSU/month between profiles 2-18 (straight line), and then a rapid degradation for later profiles. The dashed line represents the corresponding offset in sound speed c caused by S, reaching almost 1 m/s for the last profile.

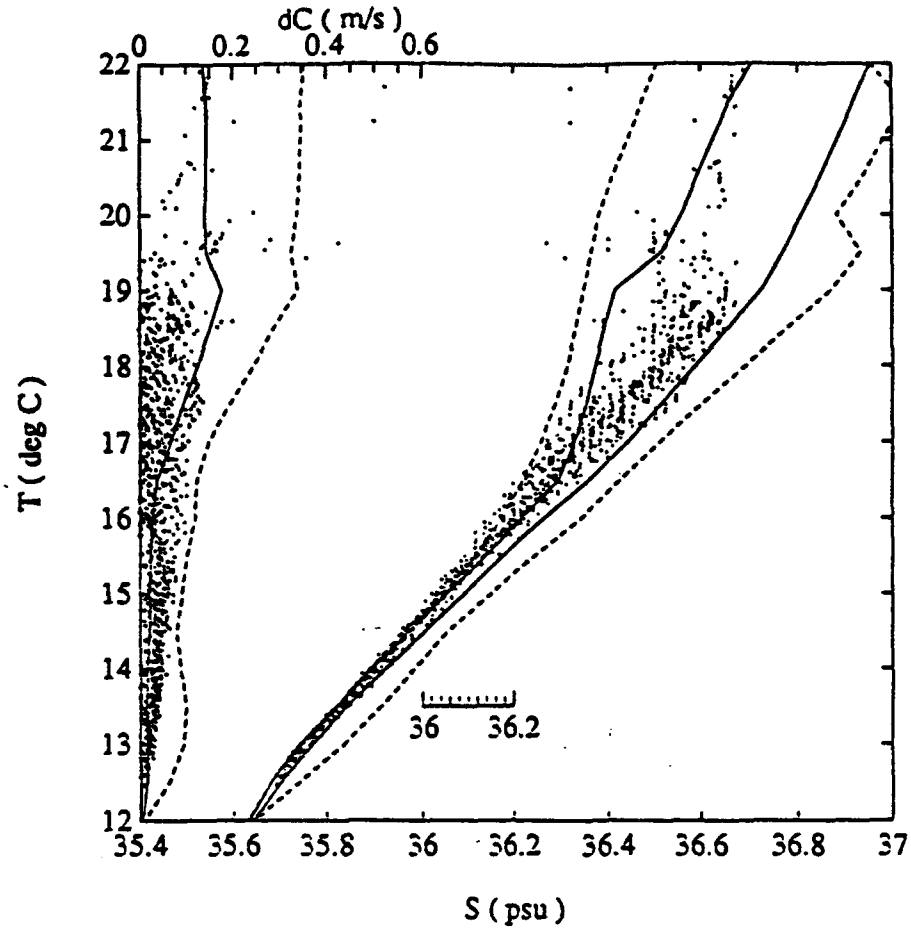

Fig. 8 The envelope of Levitus T-S curves are computed following the CTD-ALACE track (Fig. 3). The solid lines represent the envelope of the seasonal curves (Levitus T-S values interpolated to ALACE profile date). The dashed lines are computed using all four Levitus seasonal values, therefore representing annual variability. CTD-ALACE T-S values, with S corrected for offsets in Fig. 7, are shown for the first 18 profiles (dots). The offset correction forces agreement for deep values, while still preserving the shape, and variability, within each individual profile. Resolution of S transmitted through Argos is 0.02 PSU. Taking the mean T-S Levitus curve (computed from the seasonal data), sound speed anomaly dc is calculated for the CTD-ALACE (dots, left-hand side of plot, absolute values shown). Maximum dc values are also computed for the Levitus (seasonal, annual) T-S curves (solid, dashed lines respectively). By guessing S from the mean Levitus T-S curve, c is estimated to within 0.2 m/s for T<18°C, and 0.4 m/s for the shallow values.

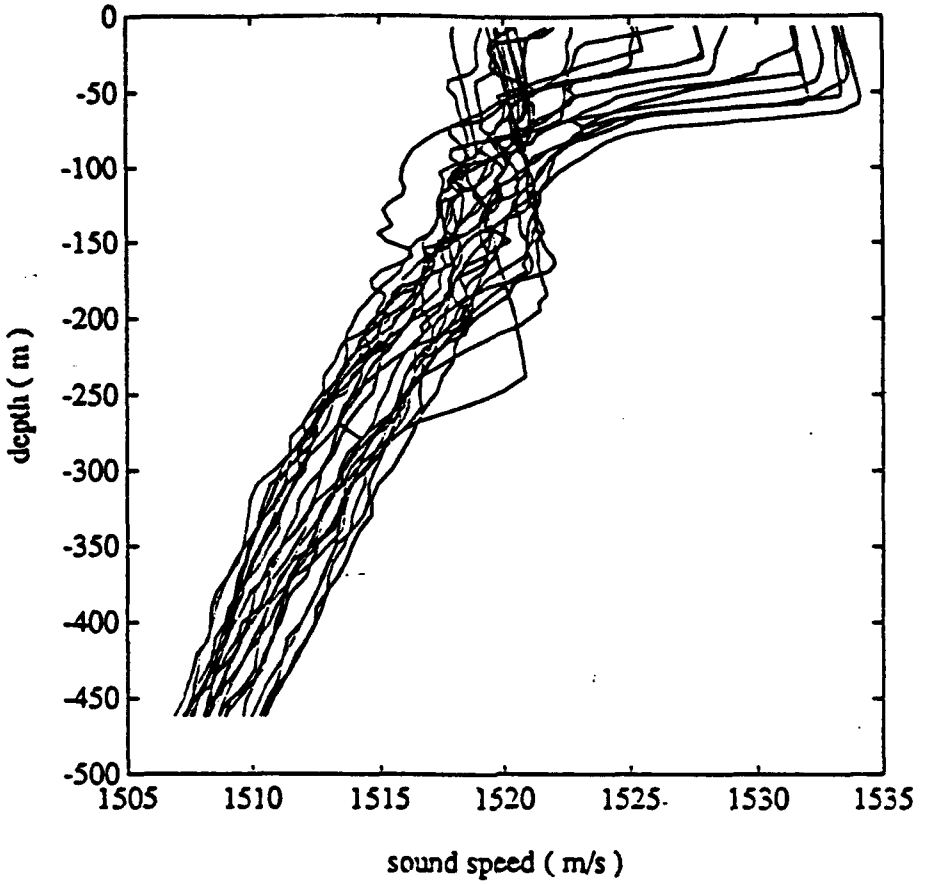

Fig. 9 Sound speed c is calculated for all 25 profiles, after correcting salinity for offsets in Fig. 7. The amount of natural variability (10 m/s in the mixed layer, 5 m/s for deep values) is due to the variance in temperature. The effect of salinity on c (Fig. 8) corresponds to ~2% of the effect by T.

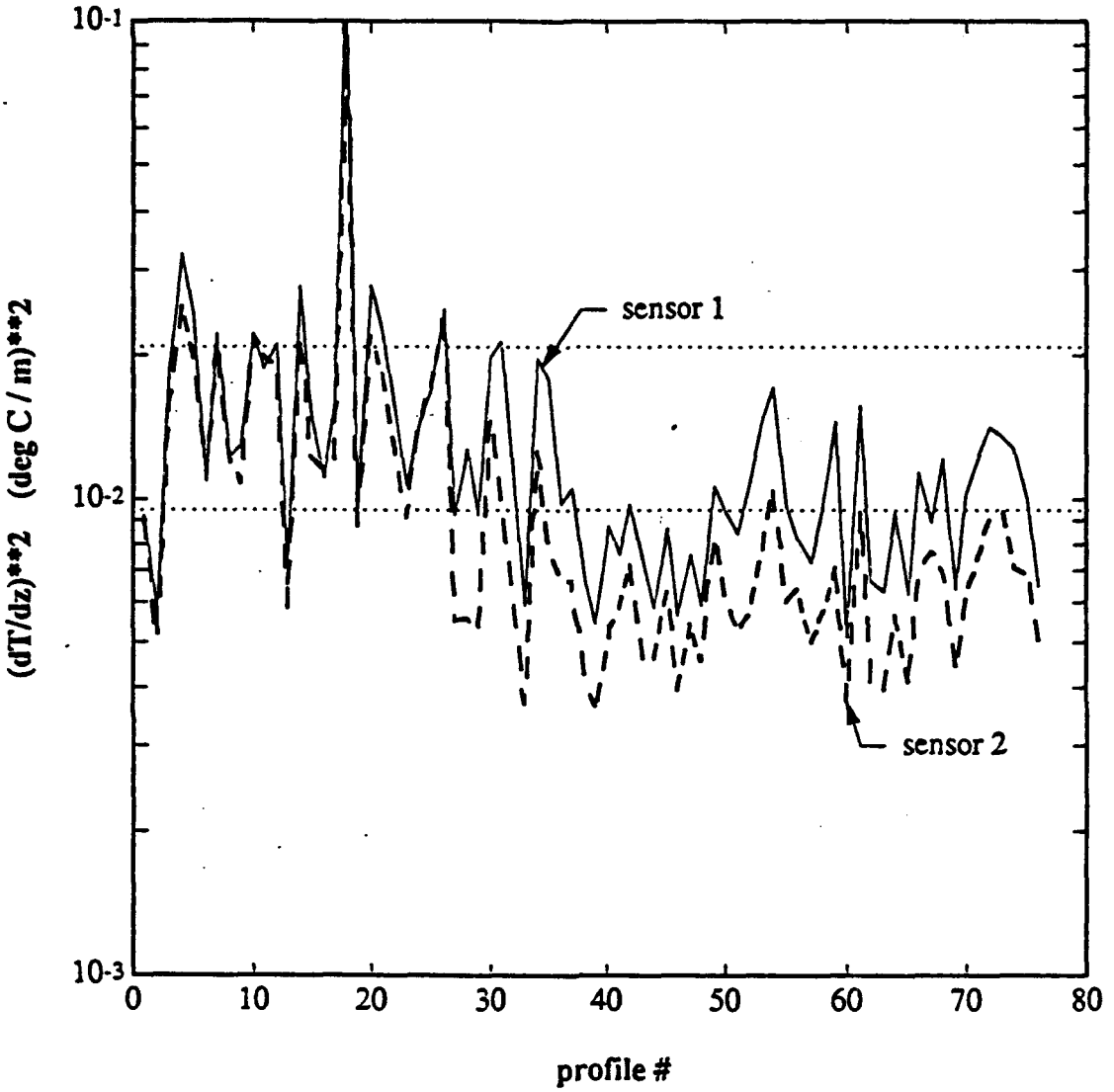

Fig. 10 $(dT/dz)^2$ is averaged for z>200 m for each profile for both sensors. After profile 26, variance of sensor 2 falls to 65% of sensor 1 for the remainder of the deployment. The average background value of dT/dz is 0.02 deg C/m, such that $(dT/dz)^2$=0.01 corresponds to a Cox number equal to 75. The dotted lines represent 95% confidence limits on the mean value of $(dT/dz)^2$ for each profile, assuming log-normal statistics (Baker and Gibson, 1987). Thus the reduction of variance in the latter half of the cruise is statistically significant.

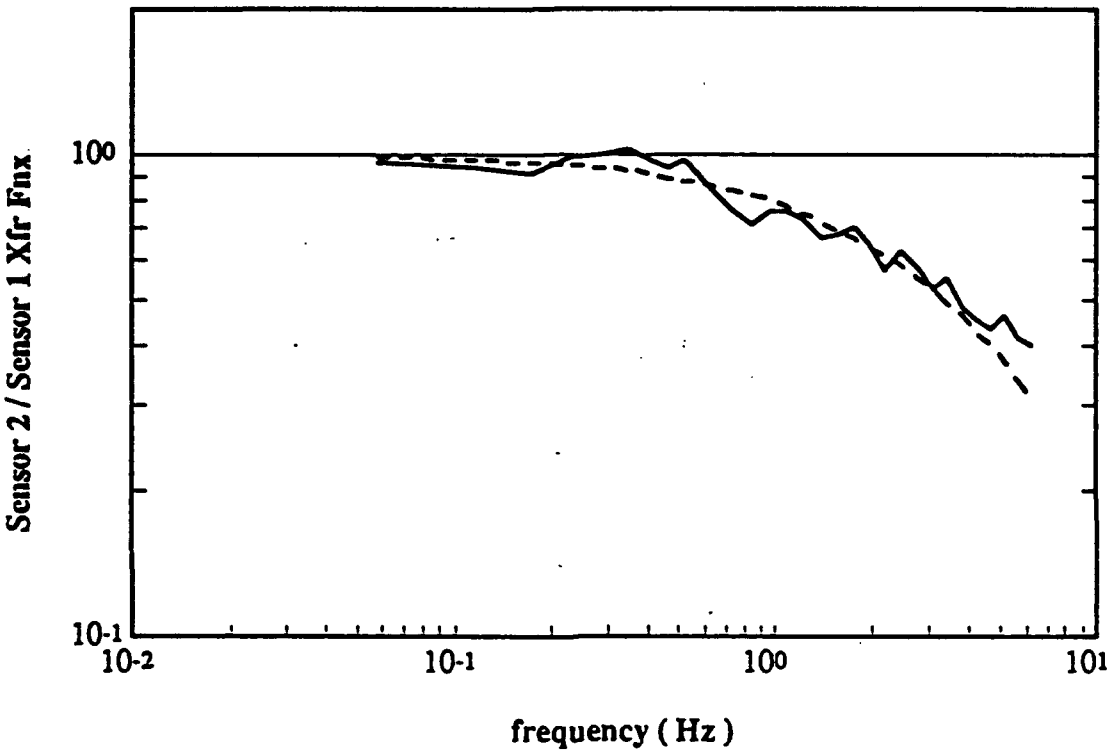

Fig. 11 The average spectrum is computed for both sensors for each profile for z>200 m. The ratio of these spectra represents a comparison of the frequency response between both probes. Change in response of probe 2 compared to probe 1 is averaged over all profiles after profile 26, where it is now attenuated at high frequencies (solid line). Behavior is similar to a single-pole filter with a -3 dB point at 8 Hz (dashed line).

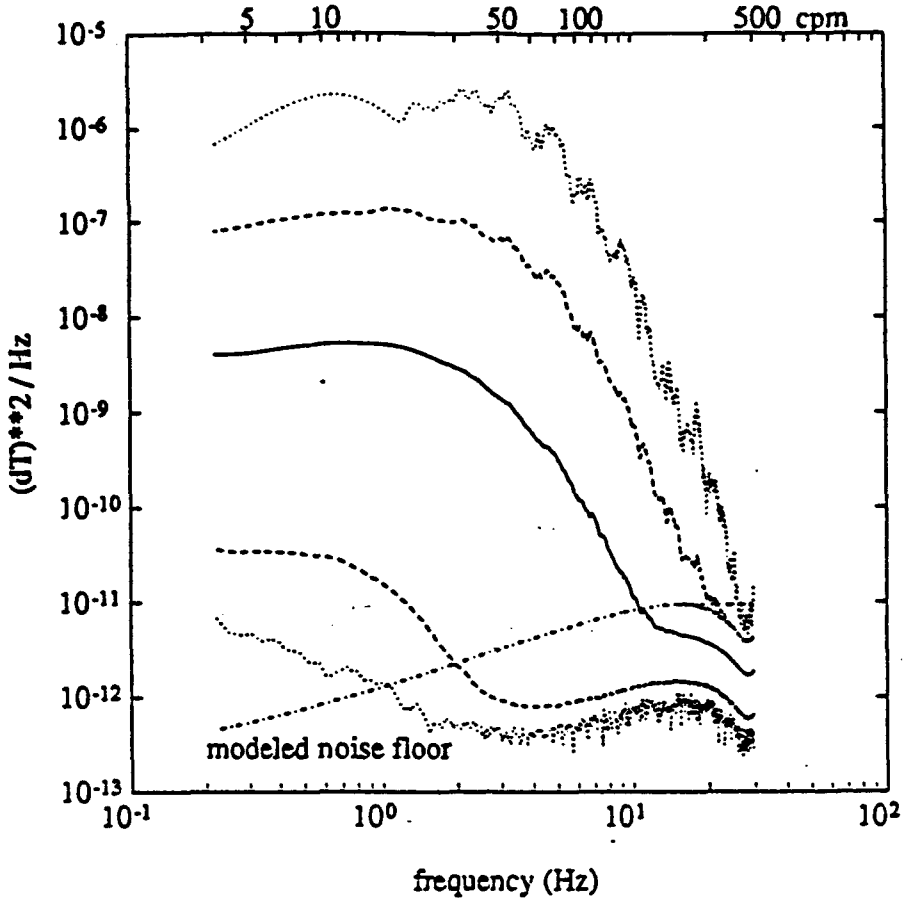

Fig. 12 The average dT/dz spectrum is computed over all profiles for z > 200 m (solid line). The maximum and minimum spectral values for each profile is also averaged over all profiles (dashed lines). Additionally, the maximum and minimum values inclusive of all profiles is found (dotted lines). The profile-averaged minimum spectrum is used to model the shape of the noise floor (dash-dot), with its level set by the maximum spectrum level, effectively setting the upper limit of the noise floor. For simplicity, the noise floor is modeled as a constant level for f>15 Hz. When an individual spectrum falls below the modeled noise floor, all higher frequencies are considered to have low SNR, and their spectral levels are set to zero. Thus $(dT/dz)^2$ variance is estimated using only the lower wavenumbers, where there is good SNR. Given the average fall rate of 6 cm/s, f=6 Hz is equivalent to k=100 cpm.